THE PUBLISHING HOUSE
OF THE ROMANIAN ACADEMY

PROCEEDINGS OF THE ROMANIAN ACADEMY, Series A,
Volume 22, Number 2/2021, pp. 177–184

NUMERICAL SIMULATION OF TAILORED HYBRID BLANKS

Ozan SINGAR[1], Dorel BANABIC[2]

[1] Daimler AG, Sindelfingen Germany
[2] Technical University of Cluj-Napoca, Romania
Corresponding author: Ozan Singar, E-mail: ozan.singar@daimler.com

Abstract. In times of resource scarcity issues energy efficiency and lightweight design in automotive construction are often in discussion. Thus, integration of lighter materials such as aluminum or composite materials in vehicle structures can recently be found. To save weight and costs, the use of tailor welded blanks consisting of metal sheets with different thicknesses or qualities are increasingly installed. As a novel concept of tailor welded blanks, different material combinations for example steel and aluminum are in research. However, the increasing use of simulations tools to accelerate the product development cycle brings new challenges for innovative joining processes. The main aim of this study is to generate a simulation model of hybrid blanks which includes the material properties of the Cold Metal Transfer (CMT) weld line as well. Four-point bend tests were performed to verify the proposed numerical model. Different finite element models for the hybrid tailor welded blanks (TWB), i.e. a shell and solid element without Heat Affected Zone (HAZ), solid element with HAZ, and last but not least a mix of shell-solid element with considering the HAZ was compared in terms of accuracy. The results show that the generated weld seam can describe the stiffness of the CMT hybrid weld.

***Key words**:* Cold Metal Transfer welding, simulation, aluminum steel tailored hybrid blanks.

1. INTRODUCTION

The scarcity of resources of fossil fuels and increasing environmental awareness of the modern society lead to the fact that car manufactures are increasingly searching for alternative materials and manufacturing methods. For this reason, lightweight metals such as e.g. aluminum combined with steel can be found increasingly in the car structure. A possibility to consult steel-aluminum hybrid structures is the use in form of tailor welded blanks. Toshiaki et. al. [1] investigate the weldability with 3D shape weld line by using friction stir girth welding between aluminum (AA6063) and steel (S45C) rods with 53 mm in diameter. It was difficult to fabricate defect free weld without tool tilt angle. The welding force and temperature increased with rotating angle of weld material. These increased the area of HAZ and softened the microstructure of the weld. Compared with conventional Friction steer welding tools, a friction stir scribe tool can reduce heat input significantly limiting the IMP Layer Thickness. Defect free lap weld joint of AA6022 and DP600 was achieved by friction stir scribe technology. However, experimental results show welds broken at the loading side of Al with IMP layer thickness of 350−750 nm [2]. Effect of pin length on Friction Stir Spot welding (FSSW) of Aluminum-Steel joints can be found in [3]. FSSW was done by changing the pins length between 0.65 mm and 1.5 mm. The maximum tensile load increased when the tool penetration depth goes up and the pin length decreased.

In the last years, Cold Metal Transfer (CMT) welding is considered for joining aluminum and steel. The characteristic of the Al-St CMT seam is a weld braze. The aluminum edge is melted while creating a solder joint on the steel surface. A prerequisite for the joining of aluminum and steel with the CMT process is according to Jank et al. [4] the use of a galvanized steel sheet. To ensure adequate wetting of the aluminum on the steel sheet, a zinc layer thickness of about 10 μm is recommended. Bruckner et al. mention in [5] that through numerous trials, compared to electrolytic galvanized steel sheets (+ ZE), pure hot-dip galvanized coil-coated zinc coatings (+ Z) are by far the most suitable for an Al / St compound. In contrast, galvanic coated (+ ZA) steels are not suitable for use. In the further course of the work a continuing development of

the company Voestalpine is presented. By a special geometrical adaptation of the joining edges such as the rolling of the steel edge and the notch of the aluminum edge, it is possible to produce a quasi-butt seam. This arrangement showed a massive reduction in surface corrosion in corrosion studies compared to an overlap joint. In [6] on AW5182-H111 / DX54D + Z CMT welded blanks, it is proved that the residual stresses in the top and bottom of the seam are due to a symmetrical weld geometry, which is achieved by welding both sides with the parameter setting $v_S = 60$ cm/min, $v_D = 4{,}5$ m/min, $I = 70$ A, $U = 12$ V and $f = 70$ Hz, equally restrained. In general, the measurement shows a typical residual stress state at welds without phase transformation. A comparative study by Pinto et al. shows in [7] that the reduced heat input in the CMT process reduces the expansion of the heat affected zone and reduces the resulting residual stresses at the weld compared to the pulsed MIG or laser hybrid welds on Al / St boards.

Singar and Banabic [8] determined in first fundamental experiments the mechanical properties by means of a tensile test, microhardness measurements and a prototype for an application of THB welded by the CMT Technique. Due to the material and thickness ratio between steel or CMT seam and aluminum no significant plasticization is recorded in the steel sheet and in the area of the CMT seam. All specimens failed beyond the HAZ in the aluminum which leads to the result of no impact of quality irregularities inside of the CMT to the stress behaviour. The hardness of this zone varies between the hardness of the aluminum base material and the hardness of the welding zone, which is under 100 HV. Optical micrographs present a weld width of approx. 2.4 mm and a total length beginning from aluminum welding area to ending steel brazing area of approx. 7 mm. The determination of the HEZ of the weld seam shows that the thermally influenced zone lies within the weld seam and shows no significant expansion in the direction of the aluminum base material. The results of microhardness testing across the weld seam show that constant mechanical properties in the seam thickness direction can be used regarding the modelling of the CMT seam. Further application of CMT Welding reported by various authors can be found in [9].

While tailored blanks of steel are used in many different components of the body shell, Tailored Hybrid Blanks (THB) are still in the development phase. To introduce the THB in car structures, careful examinations regarding forming characteristics and mechanical properties of hybrid blanks should be carried out. The production and processing of THB are time consuming and expensive. Thus, Finite Element Modelling (FEM) of hybrid blanks is essential to prevent the risk of wrong application. There are two strategies to model the tailor hybrid blanks. The first strategy is to model the different blanks without the weld line. In the study of Meinders et al. [10] the weld line itself did not modelled but represent a simple boundary condition between the base materials. On the other hand, the second strategy takes the weld line into account. Zhao et al. [11] analysed different modelling types (without weld, with weld: shell, solid) of steel tailored blanks. It is recommended to use a shell element model in simulation of steel TWB due to the advantage of much less computing time compared to solid elements. The study of Padmanabhan et al. [12] shows the deep drawing simulations of aluminum-steel tailored blanks. In this research, the rule of mixture is used to describe the material behaviour of the weld line. Results represent that the weld line by itself does not have significant impact on the formability due to the small size and the large gradient in mechanical properties between the sheet blanks. Extensive research has been carried out to model tailored blanks in consideration of the weld line. A simulation model for THB which was welded by the Cold Metal Transfer (CMT) welding technique has not been fully examined and developed.

In the present paper, a novel modelling technique of the THB including the precise geometry and material properties of the CMT weld is presented.

2. DETERMINATION MECHANICAL PROPERTIES FOR THE SIMULATION

2.1. Main characteristic

The CMT-welding process is described in [4]. This special joining method leads to an Intermetallic Phase (IMP) seam of a few micrometers, due to the low heat input during the welding process [13]. Fig.1 shows the typical CMT cross section. The weld line has two basic characteristic compounds: welded on the aluminum plate and brazed on the steel side. The requirement for a brazing connection on the steel plate is a zinc coat layer on both sides. In addition, all test specimens have the special patented butt joined geometry from Voestalpine with its characteristic wedged steel plate end [5].

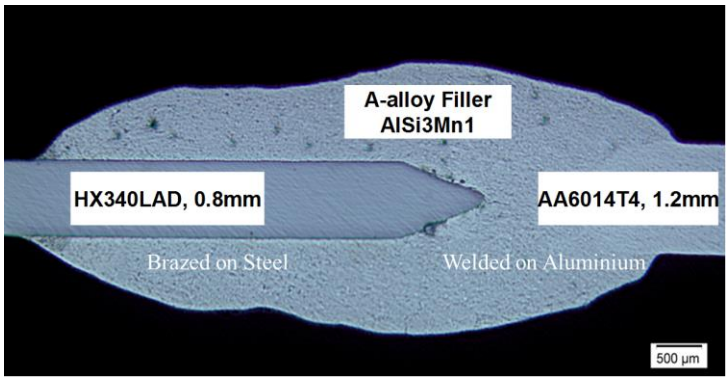

Fig. 1 – Cross-section of a CMT hybrid joint.

2.2. Mechanical properties of the weld seam

The microhardness measurement is used to indicate the occurrence of possible changes in the local material specific properties caused by thermal influences. Fig. 2 illustrates the microhardness of the CMT-weld for THB which was determined by the Vickers method. The hardness is obtained by measuring the impression surface and the corresponding force, Eq. (1). In order to avoid distortion, the samples were clamped during the welding process [7]:

$$HV = 0{,}102 \cdot \frac{2F \cdot \sin\left(\frac{136°}{2}\right)}{d^2} \approx 0{,}1891 \cdot \frac{F}{d^2}. \tag{1}$$

Results show changes in the material properties at the Heat Affected Zone (HAZ) of the CMT weld which is less than 1 mm. The results of the microhardness measurement are not able to describe the flow behaviour of the welding zone. Another way, besides the tensile test to obtain the necessary flow curves for the simulation, is the compression test. Four specimens were cut off according to the scheme shown in Fig. 3. The welding zone exists of a mix of the filler Material $AlSi_3Mn_1$ and the welded aluminum AA6014-T4. All four specimens were compressed in direction of the weld seam axis. Fig. 3 presents the stress strain curves of the tested specimens. As can be seen, only the plasticity between $0 \leq \varphi \leq 0.20$ can be used to obtain the flow behaviour of the welding zone. Up to $\varphi = 0.20$ the friction effect occurs.

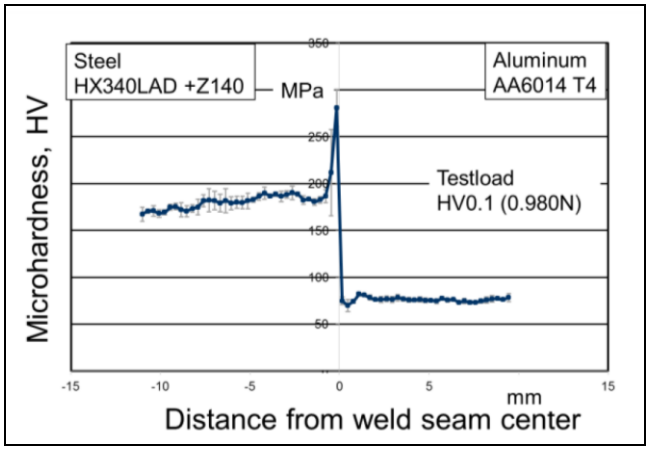

Fig. 2 – Microhardness measurement.

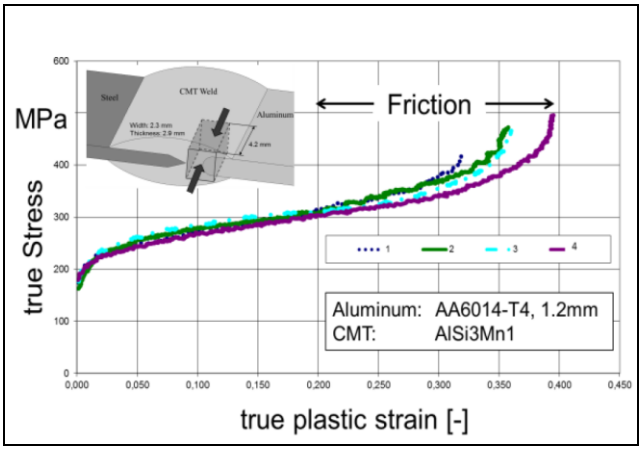

Fig. 3 – Stress-Strain curves.

Fig.4 presents the approximation of the flow curves of the welding zone. The elastic material behaviour was assumed for the CMT weld and for the basic material aluminum as linear elastic and isotropic. Therefore, the determined material parameters of the base material aluminum are adapted to describe the flow behaviour of

the CMT-weld. The approximated Hocket-Sherby curve of the basic material AA6014T4 was used and scaled for the weld flow properties by means of the following equation:

$$k_f(\varphi)_{Weld} = k_f(\varphi)_{AA6014T4} \cdot \frac{HV_{Weld}}{HV_{AA6014T4}}. \tag{2}$$

As mentioned previously, due to the small dimensions of test specimens and the influence of friction, only the beginning of the flow curve can be roughly approximated. Nevertheless, the new adapted flow curve is able to describe the welding zone plasticity, because, as mentioned above, both materials (CMT weld and aluminum) are defined as linear elastic and isotropic. One of the failure criterions for both is described by ductile normal fracture which will be discussed in the next chapter.

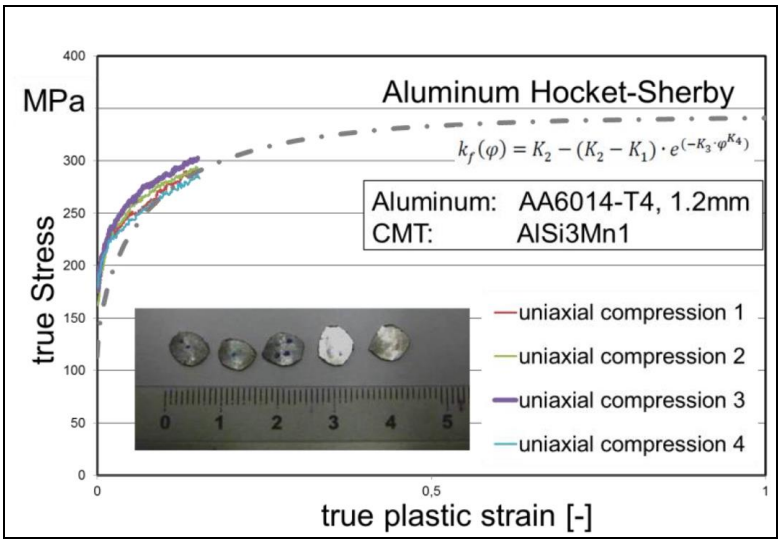

Fig. 4 – Approximation of the CMT flow curves.

2.3. Mechanical properties of the tailor hybrid blanks

In order to determine the elongation at fracture in plane strain, a three points bending test was carried out. The principle of the test is illustrated in Fig. 5. Rectangle specimens with a width of 28 mm and a length of 50mm were cut out from the tailored hybrid blanks. During the test, the bending axis is perpendicular to the weld line. The specimen is not clamped; in addition, the punch acts directly to the weld line until fractures occur. Fig. 5 right shows the result of the three points bending test. As presented, all 5 specimens failed directly in the weld line. The results were used to determine the ductile normal fracture parameters of the weld line. The existing fracture curve for the basic material aluminum AA6014-T4 was scaled by means of the three points bending test for the CMT-weld line. The fracture in plane strain defines the β-Model. According to this model, the fracture strain is a function of the parameter β which is determined as following: *s*, *d* and *q* are material parameters of the basic material aluminum. Fig. 6 presents the normal fracture diagrams for aluminum and for the CMT weld. The CMT ductile normal fracture curve was obtained by scaling basic aluminum ductile normal fracture curve.

$$\beta = \frac{1 - s\eta}{\nu} \quad \text{with} \tag{3}$$

$$\nu = \frac{\sigma_1}{\sigma_M}, \quad \sigma_M = \text{Equivalent stress von Misses} \tag{4}$$

$$\eta = \frac{\sigma_1 + \sigma_2 + \sigma_3}{\sigma_M}, \quad \sigma_1 \geq \sigma_2 \geq \sigma_3 \tag{5}$$

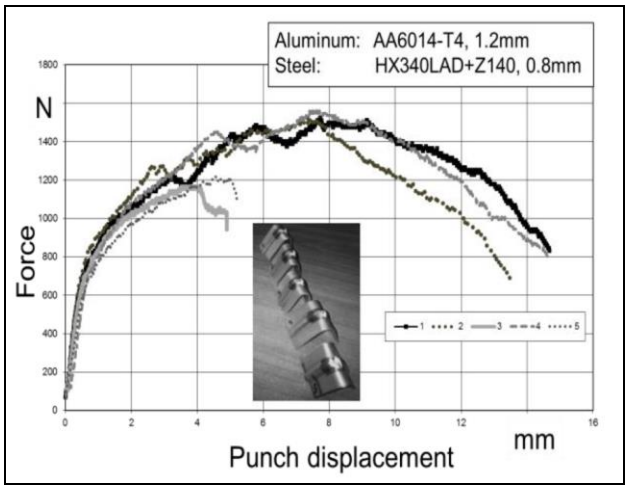

Fig. 5 – Three points bending test.

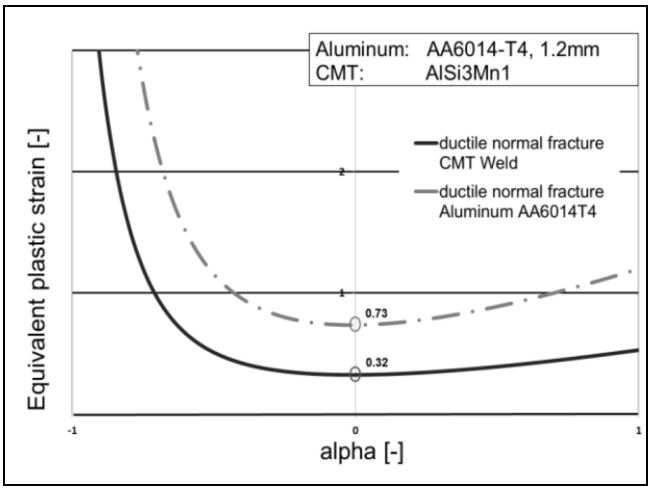

Fig. 6 – Fracture diagram for AA6014 T4 and CMT.

Four point bending test were performed to measure the stiffness of the hybrid blanks. This test is also used to verify the generated simulation model. Fig. 7 represents the schematic of test. In the area between the bearings arises a bending stress with a constant bending moment. The bending axis is compared with the three points bending test perpendicular to the weld line. The upper side of the specimen is loaded with compressive stresses, the lower with tensile stresses. Fig. 7 shows the results of the four points bending test. In all of the three specimens acts a stiffness of approximately 280 N at a max. punch displacement of 15 mm. These stiffness parameters were consulted to verify the simulation which will be discussed in the following chapter.

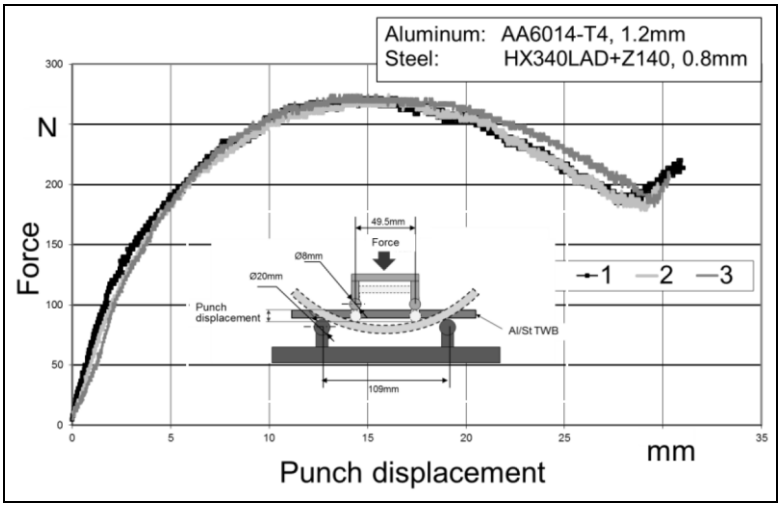

Fig. 7 – Four points bending test.

3. FINITE ELEMENT SIMULATION

3.1. Set up

In this work, two different modelling methods were investigated to create a simulation model [14]. In the simplest model as shown in Fig. 8 (1 and 2), the base materials steel and aluminum are linked together as a solid or a shell element without the weld characteristics. Second, the material properties of the weld (HAZ) are taken into account and modelled as solid and shell/solid element, Fig. 8.

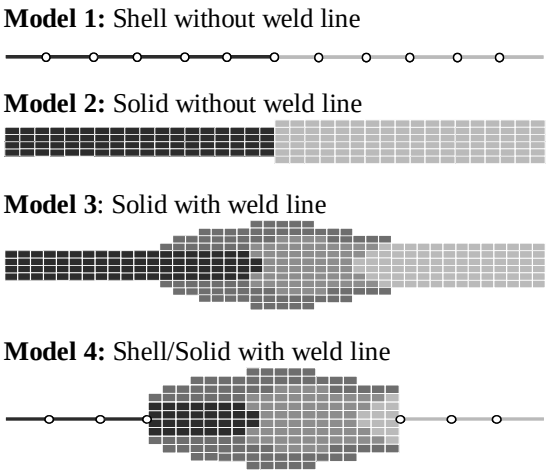

Fig. 8 – Modelling types.

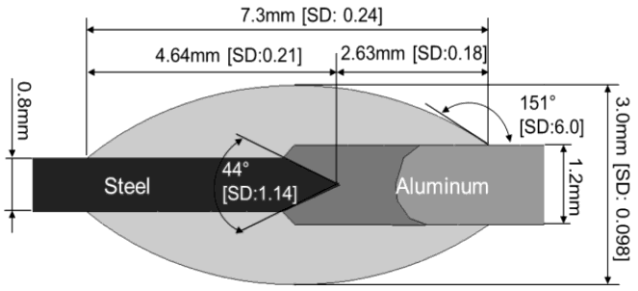

Fig. 9 – CMT Geometry.

To define the exact geometry parameters of the CMT weld and in order to implement these in LS-Dyna, the size of the weld geometry was measured by five different microscopic views on each plate. This has been done on 8 different welded tailored hybrid blanks, Fig 9. CAD models were created by the tool CATIAV5. This data linked to a finite element model in LS-PREPOST. LS-PREPOST sets the individual element size, the element type (shell or solid) and define the connection between the elements. To reduce the simulation time, the element size should be set rougher in areas with little change of displacement. A fine mesh size has been used for the CMT weld. To connect the shell/solid elements in Model 4, the command *CONSTRANED_SHELL_TO_SOLID in LS-Dyna is used which is designed to connect four node shell elements with eight-node solid elements.

3.2. Validation of the models

To validate the generated models 1-4, the four-point bending test and a Nakajima test ([15], [16]) was simulated. The simulation model of the experimental setup (punch, bearings) was considered as rigid shell element. Fig. 10 presents the validation of the models. Results of the punch force and displacement were compared with the real F-d- curves. The calculation indicates that, model 1 and model 2 which considers only the base materials has a remarkably force difference. The maximum force lies in the simulation at about 200 N, while in the real test the punch applies a force up to 275 N. The pure consideration with shell elements refers to the simulation, which contains 150 N while the model with only volume element increases the approximation minimally. The maximum deviation is at 25 %. The lower bending stiffness of the simulation is due to the missing material properties of the weld seam. However, if the weld seam is considered in the simulation a significant improvement in the calculation can be recorded. Model 3 with solid elements initially shows a good similarity compared to the curve of the real tests. After 20 mm of punch displacement the force decreases rapidly on real tests. In this case the error for the max. force is less than 1 %. The modelling of the weld seam with volume elements leads to an improvement in the quality of the result with regard to force transmission, but there is a high deviation in terms of bending stiffness. The calculated stamp path cannot be reproduced correctly in comparison to the real test, which is part of an error of up to 16 %.

The results of the combined shell/solid – model 4 are not provided due to a failed simulation calculation at the beginning. The interface between solid and shell elements defined by the command CONSTRAINED_SHELL_TO_SOLID seems to fail and offer not meaningful evaluations.

The Nakajima trial is being considered for further verification of the THB modelling techniques. Initially, experimental investigations were carried out on corresponding samples. In order to expose the CMT seam to different stress states, sample geometries recommended by the German group IDDRG were used. Figure 11 shows the distribution of the main degree of deformation φ_1 in a section plane perpendicular to the weld using the example of the plane stress state. The experimental tests show that the CMT seam moves in the direction of the steel plate with a punch height of h_p = 17.5 mm to approx. 12 mm. Due to the migration

of the weld seam, there is a main deformation with approx. $\varphi_1 = 0.35$ in the aluminum plate. Since the main stress lies in the aluminum area and in the material constriction of the board, the component failure will occur here as the forming progresses. In contrast, there is an almost constant change in shape of $\varphi_1 \approx 0.03$ in the steel material and in the transition area.

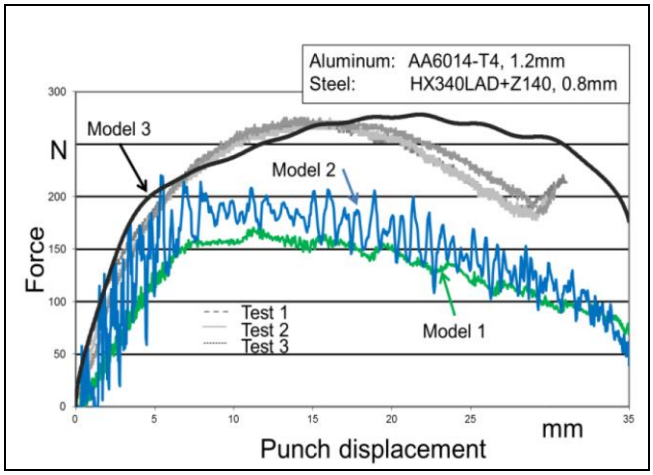

Fig. 10 – Bending Test

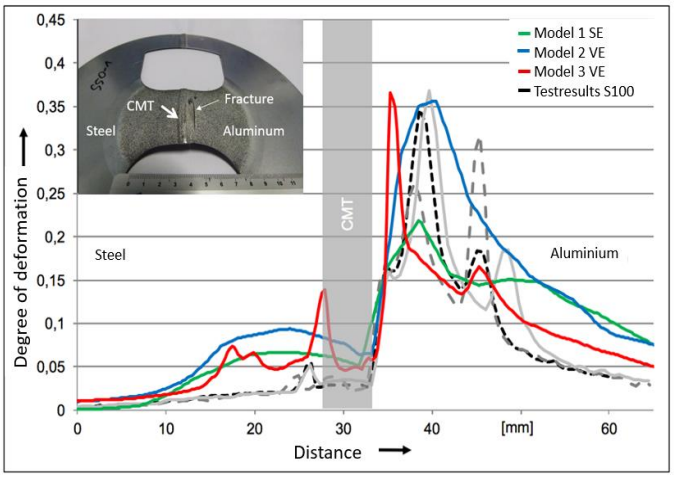

Fig. 11 – Nakajima Test

Despite the almost correct representation of the location of the main transformation of all 3 modeling types, the level of φ_1 with model 1-SE is underestimated by approx. 40%. If volume elements are used for modeling instead of shell elements, the calculation results can be clearly improved (model 1-VE; model 2-VE).

The main transformations calculated in this way are in good agreement with the experimental results. In this case, the deviation for the maximum degree of deformation is less than 3 %. Although both modeling variants precisely calculate the maximum degree of deformation, neither of the two models correctly reproduces the φ_1 curve in the areas of the base plates. The modeling variant, considering the weld seam properties (model 2-VE), tends to lead to a better distribution of elongation, but the maximum degree of deformation in the transition area is overestimated by $\varphi_1 = 0.05$ by approx. 40 %. Since the width of the CMT seam to the sample geometry is relatively narrow and thus accounts for a small share of the total volume, the consideration of the weld properties in the volume element (model 2-VE) only leads to a slight improvement in accuracy. The results described here using the example of the S100 also apply qualitatively to samples R0 and S50.

4. CONCLUSION

In this work, different finite element models for aluminum steel combinations welded by the CMT technology were developed and examined. A compression test was used to define the exact flow parameters of the flow curve. Generally speaking, the results are more precisely compared to the real tests when using the exact geometry and the material parameters of the weld seam. By comparing the experimental data, it could be shown that the consideration of the plastic weld properties in the simulation model leads to an increase in the calculation accuracy. However, with the increase in accuracy, it should be taken into account that modeling with volume elements including a complex failure description of the weld seam, results in an increase in the calculation time. However, in order to save the high computing time and the complex modeling of the CMT seam, it should be checked before the respective application whether the increase in accuracy justified. With the aim of analyzing the durability, further fatigue test should be carried out.

REFERENCES

1. Y. TOSHIAKI, W. TIAN, H. ATSUHIRO, M. TATSUYA, H. KATASHI, F. MASAHIRO, *Friction stir girth welding between aluminum and steel rods. Procedia Manufacturing*, **15**, pp. 1376-1381, 2018.
2. W. TIANHAO, S. HARPREET, S. RAJIV, H. YURI, U. PIZUSH, C. BLAIR, *Evaluation of intermetallic compound layer at aluminium/steel interferace joined by friction stir scribe technology*, Materials and Design, **174**, p. 107795, 2019.
3. M. JOAQUIN, G. HERNAN, *Effect of pin length on Friction Stir Spot Welding (FSSW) of dissimilar Aluminium-Steel joints*, Procedia Materials Science, **9**, pp. 504-513, 2015.
4. N. JANK, H. STAUFER, J. BRUCKNER, *Schweißverbindungen von Stahl mit Aluminium – eine Perspektive für die Zukunft*, Berg- und Hüttenmännische Monatshefte BHM, **153**, pp. 189-192, 2008.
5. J. BRUCKNER, E. ARENHOLZ, *Die Stahl-Aluminium-Hybridplatine – eine innovative Lösung für den Mischbau*, Deutscher Verband für Schweißen und verwandte Verfahren DVS, Gr0ße Schweißtechnische Tagung Düsseldorf, pp. 335-337, 2011.
6. L. AGUDO, S. WEBER, H. PINTO, E. ARENHOLZ, J. WAGNER, H. HACKL, J. BRUCKNER, A. PYZALLA, *Study of microstructure and residual stresses in dissimilar Al/Steels welds produced by Cold Metal Transfer*, Materials Science Forum, **571-572**, pp. 347-353, 2008.
7. H. PINTO, A. PYZALLA, H. HACKL, J. BRUCKNER, *A comparative study of microstructure and residual stresses of CMT-, MIG and laser-hybrid welds*, Materials Science Forum, **524-525**, pp. 627-632, 2006.
8. O. SINGAR, D. BANABIC, *Characterization and application of tailored hybrid blanks*, Romanian Journal of Technical Sciences – Appl. Mechanics, **65**, *1*, pp. 37-52, 2020.
9. S. SELVI, A. VISHVAKSEN, E. RAJASEKAR, *Cold metal transfer (CMT) technology – An overview*, Defence Technology, **14**, pp. 28-44, 2018.
10. T. MEINDERS, A. VAN DER BERG., J. HUÉTINK, K. BENEDIKT, *Deep drawing simulations of Tailored Blanks and experimental verification*, Journal of Materials Processing Technology, **103**, pp. 65-73, 2000.
11. K.M. ZHAO, B.K. CHUNG, J.K. LEE, *Finite element analysis of tailor-welded blanks*, Finite Elements in Analysis and Design, **37**, pp. 117-130, 2001.
12. R. PADMANABHAN, M.C. OLIVEIRA, L.F. MENEZES, *Deep drawing of aluminium-steel tailor welded blanks*, Materials and Design, **29**, pp. 154-160, 2008.
13. L.J. AGUDO, D. EYIDI, C.H. SCHMARANZER, E. ARENHOLZ, N. JANK, J. BRUCKNER, A.R. PYZALLA, *Intermetallic FexAly-phases in a steel/Al-alloy fusion weld*, Journal of Material Science, **42**, pp. 4205-4214, 2007.
14. D. BANABIC, *FE-models of the sheet metal forming processes*, In: *Sheet metal forming processes: constitutive modelling and numerical simulation* (ed. D. Banabic), pp. 1-25, Springer, Heidelberg, 2010.
15. D. BANABIC, *Anisotropy and formability of AA5182-0 aluminium alloy sheets*, Annales of CIRP, **53**, pp. 219-222, 2004.
16. A. KAMI, B. MOLLAEI DARIANI, A. SADOUGH VANINI, D.S. COMSA, D. BANABIC, *Application of a GTN damage model to predict the fracture of metallic sheets subjected to deep-drawing*, Proceedings of the Romanian Academy, Series A, **15**, *3*, pp. 300-309, 2014.

Received October 16, 2020